





## Peelable porous nanosheet fabricated by roll-to-roll coating and nanoimprinting technique

**Takuto Aoki**, Course of Science and Technology, Graduate School of Science and Technology, Tokai University, 4-1-1 Kitakaname, Hiratsuka, Kanagawa 259-1292, Japan

**Tomomasa Suzuki**, Course of Applied Science, Graduate School of Engineering, Tokai University, 4-1-1 Kitakaname, Hiratsuka, Kanagawa 259-1292, Japan

**Yuta Sunami**, Department of Mechanical Engineering, School of Engineering, Tokai University, Hiratsuka, Kanagawa 259-1292, Japan; Micro/Nano Technology Center, Tokai University, Hiratsuka, Kanagawa 259-1292, Japan

**Hong Zhang** , Micro/Nano Technology Center, Tokai University, Hiratsuka, Kanagawa 259-1292, Japan; School of Chemical Engineering and Technology, Tianjin University, Tianjin 300350, China

**Yosuke Okamura** , Course of Science and Technology, Graduate School of Science and Technology, Tokai University, 4-1-1 Kitakaname, Hiratsuka, Kanagawa 259-1292, Japan; Course of Applied Science, Graduate School of Engineering, Tokai University, 4-1-1 Kitakaname, Hiratsuka, Kanagawa 259-1292, Japan; Micro/Nano Technology Center, Tokai University, Hiratsuka, Kanagawa 259-1292, Japan; Department of Applied Chemistry, School of Engineering, Tokai University, Hiratsuka, Kanagawa 259-1292, Japan

Address all correspondence to Hong Zhang at [zhanghong@tju.edu.cn](mailto:zhanghong@tju.edu.cn) and Yosuke Okamura at [y.okamura@tokai-u.jp](mailto:y.okamura@tokai-u.jp)

(Received 12 May 2023; accepted 14 August 2023; published online: 1 September 2023)

### Abstract

A combination of roll-to-roll coating and nanoimprinting technique is proposed for large-scale fabrication of porous nanosheets. Poly (D,L-lactic acid) (PLA) in 2-methoxy-1-methylethyl-acetate is roll-to-roll coated on polypropylene substrate to obtain nanosheets with thickness above *ca.* 95 nm. Roller nanoimprinting with a nickel mold is applied to fabricate pores on nanosheets with diameter of *ca.* 1.2  $\mu\text{m}$ . The imprinted PLA nanosheets with thickness above *ca.* 129 nm can be directly peeled from the substrate using a polyester adhesive tape frame with open circle of 30 mm. This method shows promising potential for achieving continuous production of porous nanosheets to facilitate their application.

### Introduction

Live imaging allows the visualization of dynamic processes of cells and tissues in their native environment, which has become an indispensable tool for biological and biomedical research. In recent years, with the rapid development of microscope technology and fluorescence probe, a variety of cellular events at the single-molecule level have been tracked in real time.<sup>[1–3]</sup> Nevertheless, it is still a fact that the observation method in live imaging is miscellaneous and reliant much on know-how of each researcher. For instance, blood cells, different from adherent cells, are suspended in liquid media, which makes them locally unstable in imaging field, especially when an aqueous external stimulus is added. In order to track various physiological behaviors of living cells, they ought to be immobilized on the focal plane. Traditional methods for cell immobilization involve extracellular matrix or synthesized polymer coating.<sup>[4–6]</sup> For suspension cells, however, physical immobilization always induces undesirable nonspecific activation, and thus technologies such as lipid-like cell membrane anchor or microfluidic device has been developed for the observation of suspension cells.<sup>[7–10]</sup> Obviously, these methods are not adequate to investigate the cell–cell interaction or cell–matrix adhesion in the presence of blood serum, which remains a big challenge in live cell imaging.

Polymer thin film, often called nanosheet as the thickness decreases into *ca.* 100 nm scale, it exhibits high transparency,

good flexibility, and a strong physical adsorption capacity without employing adhesive glue or reactive functional groups.<sup>[11–14]</sup> The unique properties arising from the nano-thickness have endowed nanosheets with broad potentials in biomedical and healthcare applications.<sup>[15]</sup> In our previous studies for bioimaging applications, to address the issue of desiccation and motion blur that occurs during live tissue imaging, we have proposed the use of nanosheets to wrap and fix tissue samples, also called as nanosheet wrapping.<sup>[16–18]</sup> Moreover, for the live imaging of suspension cells, nanosheet wrapping has shown its promising advantages as well.<sup>[19]</sup> Specifically, porous nanosheet with a pore size of *ca.* 1  $\mu\text{m}$  (less than the size of a single cell) is fabricated. By wrapping the suspension cells with a porous nanosheet, a hydrodynamically stable environment can be obtained for these cells, and thus the cell response upon adding of external stimulus can be well tracked. With this method, imaging of not only the whole activation process on a specific suspension cell but also cell–cell interaction in the imaging field is possible, which cannot be achieved with any existing cell immobilization methods.

The porous nanosheet for wrapping a sample in bioimaging applications is a disposable material, and thus there is a significant need for a large quantity of nanosheet. However, the preparation of porous nanosheet is still cumbersome and costly. The most commonly used spin coating method is only applicable for intermittent and small scale fabrication.<sup>[11,12]</sup> To

obtain nanosheet in a freestanding state, a water-soluble sacrificial layer is always introduced prior to coating and a water immersion process is needed to detach the nanosheet from substrate, which further hinders the development of continuous production. Recently, roll-to-roll coating is applied to fabricate nanosheets, in which the solution is coated on a flexible substrate that is fed continuously from one roller to another.<sup>[20–22]</sup> Furthermore, combined with polymer blend phase separation method, porous nanosheet can be massively fabricated.<sup>[23]</sup> While phase separation-assisted nanofabrication is a straightforward process without sophisticated equipment, in addition to water immersion for dissolving sacrificial layer, an extra solvent immersion is needed to selectively remove unwanted phase separation domains to form porous structure. What is more, to obtain perforated pores with narrow size distribution from phase separation is still a technical difficulty, and only applicable for very limited polymer candidates. Therefore, it is highly required to develop a versatile method for large-scale fabrication of porous nanosheet.

In this study, we combine roll-to-roll coating and nanoimprinting technique to fabricate freestanding porous nanosheet. Nanoimprinting has proven a feasible and efficient method to create pattern on thin films regardless of the polymer types.<sup>[24–26]</sup> Especially, roller nanoimprinting is developed based on roll-to-roll process, which could provide a continuous method.<sup>[27]</sup> In order to achieve a real continuous production, sacrificial layer-assisted lifting-off should be avoided. Here, we simultaneously take the surface energy of coating substrate and properties of coating solvent into consideration, and the as-coated nanosheet is expected to be peeled from the substrate directly. Biocompatible poly (D,L-lactic acid) (PLA) is chosen as a model polymer, and the processing parameters for obtaining peelable porous nanosheet are discussed intensively.

## Materials & methods

### Analysis on rolled coating substrate

The rolled substrates used for roll-to-roll coating are polyethylene terephthalate (PET) film (thickness: 75  $\mu\text{m}$ , Lumirror™ 75T60) and polypropylene (PP) film (thickness: 50  $\mu\text{m}$ , TORAYFAN™ 50-2500H), purchased from TORAY Industries, Inc. (Tokyo, Japan). The substrate surface energy was obtained by a static contact angle measurement and calculated using Owens–Wendt's equation,<sup>[28]</sup> where water and diiodomethane (FUJIFILM Wako Pure Chemical Co., Osaka, Japan) were chosen as test liquids. The contact angle was measured by a contact angle meter (DMe-201; Kyowa Interface Science Co., Ltd., Saitama, Japan) at room temperature (25°C) and a normal relative humidity (35% RH). The contact angle was obtained from at least ten measurements. The values are given as mean  $\pm$  standard deviation (SD).

Regarding the surface morphology and roughness of substrate, samples were attached to freshly cut silicon wafer (40  $\times$  40 mm<sup>2</sup>, SEIREN KST Co., Fukui, Japan), and then examined using a white light interferometric microscope

(BW-S507, Nikon Co., Tokyo, Japan) with a 20 $\times$  Mirau interferometry objective (NA: 0.40, WD: 4.7 mm). The scan range and step were set to be  $\pm$  20  $\mu\text{m}$  and 20 nm, respectively, and a median filter (threshold: 200 nm,  $n=30$ ) was used to remove abnormal values. Then, the morphology of the PP film was observed with a field emission scanning electron microscope (FE-SEM, JSM-7100F, JEOL Ltd., Tokyo, Japan) at an accelerate voltage of 3 kV. Prior to observation, the sample surface was sputtered with platinum by an ion sputtering machine (SC-701 Sanyu Electron Co., Ltd., Tokyo, Japan) with conditions of 3 mA and 60 s.

### Preparation of peelable porous nanosheet

Poly (D,L-lactic acid) (PLA) pellet was purchased from NatureWorks LLC, USA, with a commercial name of Ingeo™ 4060D ( $M_w = 100\text{--}200$  kDa, 12.0 mol% D-lactide content). PLA from NatureWorks is a biopolymer which is produced by polymerization of the lactic acid that is produced by fermentation from plant derived sugars. Ingeo™ 4060D is an amorphous polymer with glass transition temperature of 55–60°C and seal initiation temperature of 80°C, designed for use in the production of oriented films, cardstock, and graphic arts, especially for heat seal layer. Ethyl acetate and 2-methoxy-1-methylethyl acetate (PGMEA) were chosen as coating solvents, obtained from FUJIFILM Wako Pure Chemical Co., and Kanto Chemical Co., Inc. (Tokyo, Japan), respectively. PLA was dissolved in a certain solvent with different concentrations, and coated on rolled substrate using a roll-to-roll coating machine (reverse gravure coating,  $\mu$ -Coater™ 350, Yasui Seiki Inc., Kanagawa, Japan). The film line speed (also called web speed) was set at 1.0 m/min with micro gravure roll speed at 16 rpm, and a furnace temperature of 100°C.

To fabricate porous structure on nanosheet, roller nanoimprinting technique was applied. The mold for imprinting is a hard nickel plate with an annular array of cone structures, which was kindly donated by JVCKENWOOD Creative Media Co. (Kanagawa, Japan). The height and bottom diameter of each cone were *ca.* 0.85 and 0.80  $\mu\text{m}$ , respectively, and the pitch distance was *ca.* 6.0  $\mu\text{m}$ . Low adhesion tape (Gelpoly® GPH100E82A04, thickness: *ca.* 150  $\mu\text{m}$ , Panac Co., Ltd., Tokyo, Japan) was adhered to the back of coating substrate. On the other side, PET substrate (thickness: 75  $\mu\text{m}$ ) and chloroprene rubber sheet (thickness: 2 mm, AS ONE Co., Osaka, Japan) were adhered to the back of nickel mold. Nanoimprinting was performed on a calender machine (TC-226, Yuri Roll Machine Co., Ltd., Kanagawa, Japan). The line speed was set at 1.0 m/min, and the extrusion pressure was adjusted from 0.1 to 0.5 MPa. All of these processes were conducted at room temperature (25°C) and a normal humidity (35% RH).

### Characterization of peelable porous nanosheet

A ring-shaped frame for detaching the as-coated nanosheet from substrate and supporting nanosheet in the air was

fabricated from a polyester adhesive tape (No.315, Nitto Denko Co., Osaka, Japan). The diameter of the open circle was cut to be 30 mm by a laser cutter (Epilog Zing 16, Epilog Laser Co., CO, USA), in which an air-cooled CO<sub>2</sub> laser tube with 30 W power is digitally controlled. After trial and error for parameter adjustment, the speed and power were determined to be 25% and 10% (based on the Epilog printing settings), respectively, and the process was performed in a raster mode with 200 dots per inch (DPI). With inappropriate parameters, the adhesive tape cannot be fully cut or gets burned. After peeling, the nanosheet was transferred on the surface of freshly cut silicon wafer. The thickness of nanosheet was determined by a scalpel scratch made on the films and measured using a stylus profilometer (DektakXT, Bruker, MA, USA). The stylus radius was 2 mm with a line resolution of 0.067  $\mu\text{m}/\text{pt}$ , and the stylus force was set to be 3 mg. The values are given as mean  $\pm$  SD. Nanosheet was also transferred on an Anodisc<sup>TM</sup> membrane (pore size: 0.1  $\mu\text{m}$ , GE Healthcare, IL, USA) and observed with SEM, using the same procedure as described above.

The roll-to-roll coating, nanoimprinting, white light interferometric microscope and SEM observation, peeling test, and nanosheet thickness measurement were performed at least three times to ensure the reliability of this study, and the representative results were presented.

## Results and discussion

### Selection of rolled substrate

PET and PP are two most commonly used rolled substrates for roll-to-roll coating. First, the usability of PET and PP rolled substrate was investigated. The static water contact angle for the two substrates was measured to be  $67.2 \pm 0.8^\circ$  and  $101.3 \pm 0.6^\circ$ , respectively (Figure S1). Similarly, contact angles of diiodomethane were  $22.2 \pm 1.8^\circ$  and  $53.2 \pm 1.4^\circ$ . According to Owens–Wendt's equation,<sup>[25]</sup> the surface energy of PET and PP substrate was calculated to be  $50.2 \pm 0.5$  and  $33.4 \pm 0.9$   $\text{mN}/\text{m}^2$ , as shown in Table I. PET with the ester group in polymer chain exhibits a higher surface energy. Due to the similar structure of PET and PLA, it is reasonable to assume that the interfacial interaction between PET and PLA is somewhat strong, and it would be difficult to directly peel PLA nanosheet from PET substrate. The surface energy of olefin PP, however, is sufficiently low as that of fluoropolymer and silicone resin. One of the objectives of this study is to prepare nanosheet that can be detached from substrate by direct peeling. PP rolled substrate

**Table I.** Contact angle of water or diiodomethane on a PET and PP substrate, and the calculated surface energies.

Polymer substrate	Contact angle (deg)		Surface energy ( $\text{mN}/\text{m}^2$ )
	H <sub>2</sub> O	CH <sub>2</sub> I <sub>2</sub>	
PET	$67.2 \pm 0.8$	$22.2 \pm 1.8$	$50.2 \pm 0.5$
PP	$101.3 \pm 0.6$	$53.2 \pm 1.4$	$33.4 \pm 0.9$

with a lower surface energy was thus chosen for the following studies.

In addition to surface energy, the surface roughness would determine whether the as-coated nanosheet can be peeled or not. Obviously, the more smooth the substrate is, the more possible the nanosheet can be peeled. The surface of PP substrate was observed using a white light interferometric microscope (Figure S2A), and the  $R_a$  roughness (arithmetic average of profile height deviations from the mean) and  $R_z$  roughness (vertical distance from the highest peak to the lowest valley) were measured to be  $6.8 \pm 1.4$  and  $36.7 \pm 13.9$  nm, respectively. Such a smooth surface provides an ideal substrate for nanosheet coating and peeling. It should be noted that a very few number of particles in micrometer scale can be observed on pristine PP substrate (Figure S2B). In order to reduce the friction between rolled substrates so that they can be easily separated from each other, inorganic anti-blocking agent is always added in commercial substrates. While the existence of such particles increases the apparent roughness of substrate, it does not cause any discomfort to nanosheet peeling, which would be shown later.

### Selection of coating solvent

Ethyl acetate and PGMEA, as good solvents to dissolve amorphous PLA, were chosen as coating solvent. The concentration of PLA solution was fixed at 25 mg/mL, and coated on PP substrate, as schematic shown in Fig. 1a. In the case of ethyl acetate, the coated film appeared cloud white as shown in Fig. 1bi, which is also called blushing defect in coating industry. In the case of PGMEA, however, the substrate was much transparent, as shown in Fig. 1ci. SEM images also confirmed that there are many holes located on the nanosheet prepared from ethyl acetate (Fig. 1bii). When using PGMEA as solvent, nanosheet became smooth and free of defects (Fig. 1cii). This finding can be attributed to the difference in the boiling point of solvent. Ethyl acetate with a low boiling point of 77.1°C exhibits a high evaporation rate. With the loss of latent heat during evaporation, the temperature of liquid layer on substrate would significantly decline, inducing the water vapor in the air condenses on the substrate, and thus craters even holes are formed after completed evaporation of solvent. The boiling point of PGMEA is 145°C, which is much higher than that of ethyl acetate. A gentle evaporation helps to avoid the temperature fluctuation and water condensation, ensuring that a homogenous and smooth nanosheet could be obtained.

### Peeling nanosheet from substrate

As discussed above, PLA nanosheet was coated on PP substrate from PGMEA solution. In order to directly peel nanosheet from substrate, various commercial adhesive tapes were tested, including Scotch<sup>TM</sup> tape, VHB<sup>TM</sup> tape, carbon tape, etc. We found that the success rate of an intact peeling depends much on the balance between adhesiveness and tape stiffness. After a careful screening, Nitto Denko No.315 tape was selected, which is a rubber-based tape with a polyester film as backing

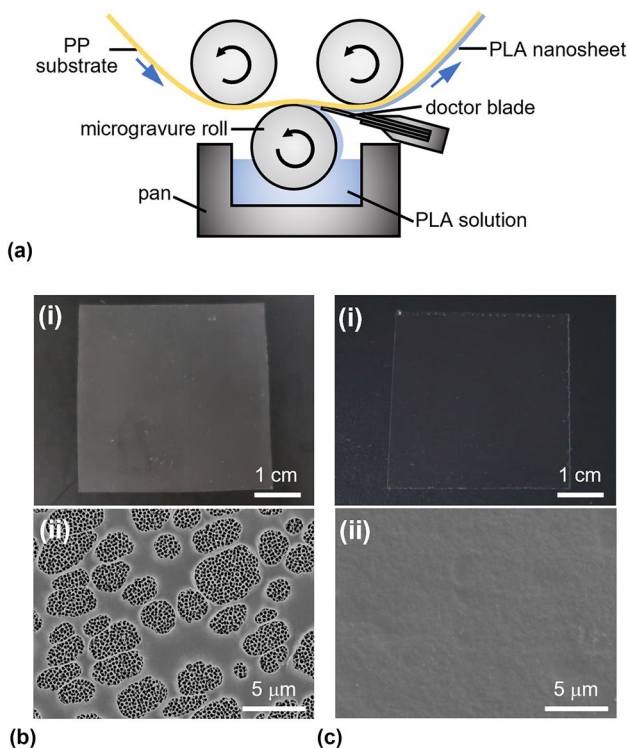


**Figure 1.** Solvent selection for fabrication of PLA nanosheet on PP substrate by roll-to-roll coating. (a) Schematic image of PLA nanosheet on PP substrate directly coated with a gravure roll. (b) Surface morphology of PLA nanosheet on PP substrate from PLA ethyl acetate solution at concentration of 25 mg/mL. (c) Surface morphology of PLA nanosheet on PP substrate from PLA PGMEA solution at the same concentration. Images (i) and (ii) show macroscopic and SEM images of PLA nanosheet transferred on an Anodisc™ membrane, respectively.

material. According to the specification provided from Nitto Denko Co., the thickness is *ca.* 85  $\mu\text{m}$ , and for a 19 mm width tape, the adhesion strength and tensile strength are 14.8 and 213 N, respectively. The tape was machined to a ring-shaped frame with an open circle of 30 mm diameter. As shown in Fig. 2a and b, we succeeded in peeling a  $128.8 \pm 2.4$ -nm-thick PLA nanosheet from PP substrate directly. Next, with increasing the concentration of coating PLA solution from 15 to 40 mg/mL, the thickness of nanosheet increased from *ca.* 95 to 1014 nm in a controllable manner, as shown in Fig. 2c. For a PLA nanosheet with thickness of *ca.* 95 nm, some cracks or holes may appear on the peeled film, which is mainly due to the inherent weak strength of a thinner film. For nanosheet with thickness above such a threshold value, a defect-free peeling can be achieved, as shown in Fig. 2d. To the best of our knowledge, this is the first report to obtain a freestanding nanosheet without the help of any liquid immersion process.

### Fabrication of porous structure

The final challenge is how to create perforated pores on nanosheet. To this end, we employed roll-to-roll method as well. Here, roller nanoimprinting technique was applied and peelable PLA nanosheet with a thickness above *ca.* 129 nm was tested. The nickel plate with an annular array of cone structures (diameter: 0.8  $\mu\text{m}$ , pitch distance: 6.0  $\mu\text{m}$ ) was used as imprinting mold. As the PP substrate prone to get twisted under extrusion, a layer of low adhesion tape was adhered to the back of substrate. Moreover, in order to ensure a homogeneous pressure distribution, a rubber sheet was adhered to the back of nickel mold. The setup is shown in Fig. 3a. After roller nanoimprinting with a line speed of 1.0 m/min and an extrusion pressure of 0.5 MPa, interference colors were shown on the surface of nanosheet, which implies the existence of a structured pattern, as shown

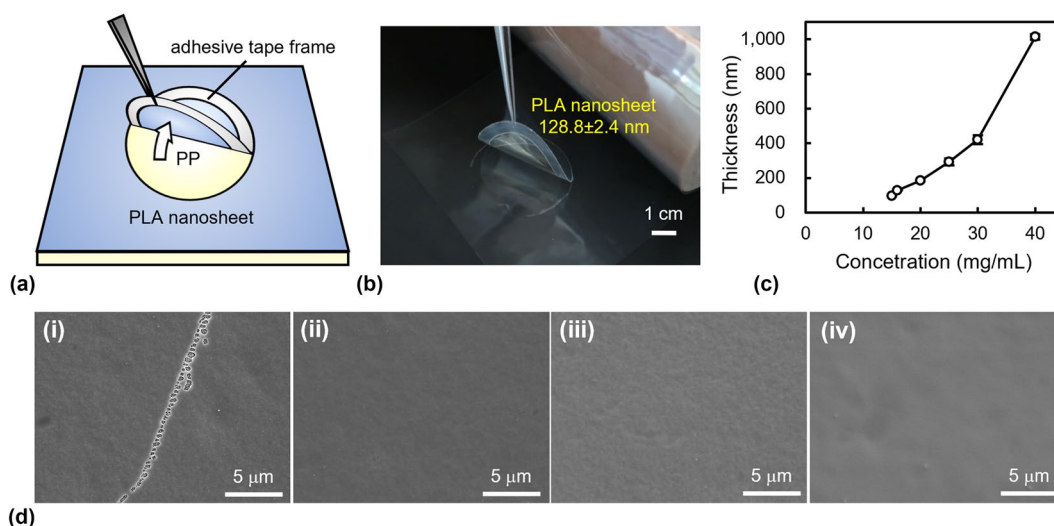


**Figure 2.** Characterization of PLA nanosheet. (a) Schematic image of PLA nanosheet detached from substrate using adhesive tape frame. (b) Macroscopic image of peeled PLA nanosheet with a thickness of  $128.8 \pm 2.4$  nm. (c) Correlation between the thickness of PLA nanosheet and the coating concentration of PLA solution. (d) SEM images of nanosheet coated from PLA concentrations of (i) 15 mg/mL, (ii) 16 mg/mL, (iii) 20 mg/mL, and (iv) 30 mg/mL.

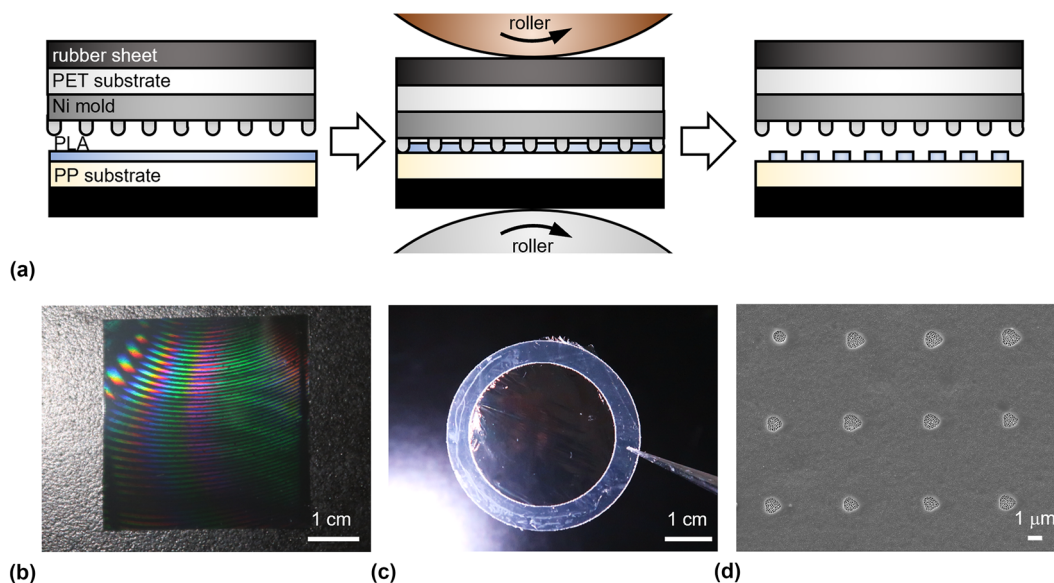


**Figure 3.** Fabrication of PLA porous nanosheet by roller nanoimprinting technique. (a) Schematic image of PLA porous nanosheet with perforated pores fabricated by roller nanoimprinting. (b) Macroscopic image of a PLA nanosheet on PP substrate after roller nanoimprinting. (c) Macroscopic image of a PLA porous nanosheet peeled and supported by the tape frame in the air. (d) SEM image of PLA porous nanosheet transferred on an Anodisc™ membrane.

in Fig. 3b. As imprinting is a mechanical punching process without any heating or irradiation treatment, we assume that the adhesiveness between nanosheet and substrate would not apparently change. With a tape frame, the imprinted nanosheet could be directly peeled from substrate as well, as shown in Fig. 3c, which supports our assumption. With increasing the extrusion pressure from 0.1 to 0.5 MPa, the area of the transferred pattern gradually increased (Figure S3). Here, we verified that an extrusion pressure of 0.5 MPa is sufficiently high to fabricate perforated pores on *ca.* 129-nm-thick PLA nanosheet, where the pattern is in good condition and the size of pores is of the same at  $1.2 \pm 0.1 \mu\text{m}$ , as shown in Fig. 3d. We also investigated the capability of nanoimprinting in fabricating porous structure with different thicknesses. While *ca.* 181-nm-thick nanosheet showed a similar pattern as that of *ca.* 129-nm-thick nanosheet, pores on *ca.* 293 nm nanosheet seemed incomplete and not perforated (Figure S4). We reason that the indentation depth under 0.5 MPa is not sufficient for *ca.* 293 nm nanosheet. It worth noting that the maximum pressure that the calender machine used in this study can provide is 0.5 MPa. If extrusion pressure is increased, it is reasonable to expect perforated porous nanosheet with a larger thickness can be fabricated. Taken together, we achieved to massively fabricate peelable porous nanosheet with roller nanoimprinting, and verified that to obtain perforated pores on thicker nanosheet, a higher extrusion pressure is required.

## Conclusions

In this study, we combined roll-to-roll coating and nanoimprinting technique to prepare porous nanosheet in large scale. By taking surface energy of coating substrate and

properties of coating solvent both into consideration, the roll-to-roll coated PLA nanosheet could be detached from PP substrate by direct peeling with an adhesive tape frame, which provides a continuous and low-cost method to prepare nanosheet. Without liquid immersion, a peelable nanosheet would largely increase its feasibility for various applications. Moreover, roller nanoimprinting has proven an efficient method to fabricate perforated pores on nanosheet. Unlike phase separation or other bottom-up methods, nanoimprinting is much versatile and can be applied to almost all the polymer materials. As presented in the introduction section, the insufficient supply of porous nanosheets is a major obstacle hindering their application for bioimaging. This study effectively addresses such issue and suggests that the proposed method will be of practical value in the massive fabrication of porous nanosheet. In future work, we aim to develop and assemble a mounting device with replaceable nanosheet for live cell imaging. As for tissue slice and even *in vivo* tissue imaging, the use of larger nanosheet for sample wrapping will offer a broader imaging window, which represents another challenge for future research.

## Acknowledgments

The authors wish to thank JVCKENWOOD Creative Media Co. for providing nickel molds for nanoimprinting, Technical Service Coordination Office at Tokai University, Tokai University Imaging Center for Advanced Research (TICAR), and Micro/Nano Technology Center (MNTC) at Tokai University for technical support.

## Fundings

This work was supported in part by “Brain Mapping by Integrated Neurotechnologies for Disease Studies (Brain/MINDS)” Project from Japan Agency for Medical Research and Development (AMED) (JP19dm0207087 (Y.O.)), Japan Society for the Promotion of Science (JSPS) KAKENHI JP18H04744 “Resonance Bio” (Y.O.).

## Data availability

The data that support the findings of this study are available on request from the corresponding authors.

## Declarations

### Conflict of interest

All authors declare no conflicts of interest.

## Supplementary Information

The online version contains supplementary material available at <https://doi.org/10.1557/s43579-023-00448-w>.

## Open Access

This article is licensed under a Creative Commons Attribution 4.0 International License, which permits use, sharing, adaptation, distribution and reproduction in any medium or format, as long as you give appropriate credit to the original author(s) and the source, provide a link to the Creative Commons licence, and indicate if changes were made. The images or other third party material in this article are included in the article’s Creative Commons licence, unless indicated otherwise in a credit line to the material. If material is not included in the article’s Creative Commons licence and your intended use is not permitted by statutory regulation or exceeds the permitted use, you will need to obtain permission directly from the copyright holder. To view a copy of this licence, visit <http://creativecommons.org/licenses/by/4.0/>.

## References

- S.W. Hell, *Science* **316**, 1153 (2007). <https://doi.org/10.1126/science.1137395>
- B. Huang, S.A. Jones, B. Brandenburg, X. Zhuang, *Nat. Methods* **5**, 1047 (2008). <https://doi.org/10.1038/nmeth.1274>
- M. Chalfie, Y. Tu, G. Euskirchen, W.W. Ward, D.C. Prasher, *Science* **263**, 802 (1994). <https://doi.org/10.1126/science.8303295>
- J. Yang, S. Nandi, *Int. Rev. Cytol.* **81**, 249 (1983). [https://doi.org/10.1016/S0074-7696\(08\)62340-2](https://doi.org/10.1016/S0074-7696(08)62340-2)
- C.S. Chen, M. Mrksich, S. Huang, G.M. Whitesides, D.E. Ingber, *Science* **276**, 1425 (1997). <https://doi.org/10.1126/science.276.5317.1425>
- D. Mazia, G. Schatten, W. Sale, *J. Cell Biol.* **66**, 198 (1975). <https://doi.org/10.1083/jcb.66.1.198>
- K. Kato, K. Umezawa, D.P. Funeriu, M. Miyake, J. Miyake, T. Nagamune, *Biotechniques* **35**, 1014 (2003). <https://doi.org/10.2144/03355rr01>
- Y. Teramura, S. Asif, K.N. Ekdahl, E. Gustafson, B. Nilsson, A.C.S. Appl. Mater. Interfaces **9**, 244 (2017). <https://doi.org/10.1021/acsami.6b14584>
- Y. Tanaka, M. Yamato, T. Okano, T. Kitamori, K. Sato, *Meas. Sci. Technol.* **17**, 3167 (2006). <https://doi.org/10.1088/0957-0233/17/12/S08>
- C.H. Lin, Y.H. Hsiao, H.C. Chang, C.F. Yeh, C.K. He, E.M. Salm, C. Chen, I.M. Chiu, C.H. Hsu, *Lab Chip* **14**, 2928 (2015). <https://doi.org/10.1039/C5LC00541H>
- Y. Okamura, K. Kabata, M. Kinoshita, D. Saitoh, S. Takeoka, *Adv. Mater.* **21**, 4388 (2009). <https://doi.org/10.1002/adma.200901035>
- S. Takeoka, Y. Okamura, T. Fujie, Y. Fukui, *Pure Appl. Chem.* **80**, 2259 (2008). <https://doi.org/10.1351/pac200880112259>
- T. Komachi, H. Sumiyoshi, Y. Inagaki, S. Takeoka, Y. Nagase, Y. Okamura, *J. Biomed. Mater. Res. B: Appl. Biomater.* **105**, 1747 (2017). <https://doi.org/10.1002/jbm.b.33714>
- Y. Okamura, K. Kabata, M. Kinoshita, H. Miyazaki, A. Saito, T. Fujie, T. Ohtsubo, D. Saitoh, S. Takeoka, *Adv. Mater.* **25**, 545 (2013). <https://doi.org/10.1002/adma.201202851>
- T. Fujie, *Polymer J.* **48**, 773 (2016). <https://doi.org/10.1038/pj.2016.38>
- H. Zhang, A. Masuda, R. Kawakami, K. Yarinome, R. Saito, Y. Nagase, T. Nemoto, Y. Okamura, *Adv. Mater.* **29**, 1703139 (2017). <https://doi.org/10.1002/adma.201703139>
- T. Takahashi, H. Zhang, R. Kawakami, K. Yarinome, M. Agetsuma, J. Nabekura, K. Otomo, Y. Okamura, T. Nemoto, *iScience* **23**, 101579 (2020). <https://doi.org/10.1016/j.isci.2020.101579>
- H. Zhang, K. Yarinome, R. Kawakami, K. Otomo, T. Nemoto, Y. Okamura, *PLoS ONE* **15**, e0227650 (2020). <https://doi.org/10.1371/journal.pone.0227650>
- H. Zhang, T. Aoki, K. Hatano, K. Kabayama, M. Nakagawa, K. Fukase, Y. Okamura, *J. Mater. Chem. B* **6**, 6622 (2018). <https://doi.org/10.1039/c8tb01943f>
- A. Zucca, K. Yamagishi, T. Fujie, S. Takeoka, V. Mattoli, F. Greco, J. Mater. Chem. C **3**, 6539 (2015). <https://doi.org/10.1039/c5tc00750j>
- Y. Tetsu, K. Yamagishi, A. Kato, Y. Matsumoto, M. Tsukune, Y. Kobayashi, M.G. Fujie, S. Takeoka, T. Fujie, *Appl. Phys. Express* **10**, 087201 (2017). <https://doi.org/10.7567/APEX.10.087201>
- M. Ito, T. Horii, T. Fujie, *Adv. Mater. Interfaces* **8**, 2100213 (2021). <https://doi.org/10.1002/admi.202100213>
- S. Suzuki, K. Nishiwaki, S. Takeoka, T. Fujie, *Adv. Mater. Technol.* **1**, 1600064 (2016). <https://doi.org/10.1002/admt.201600064>
- S.Y. Chou, P.R. Krauss, P.J. Renstrom, *Appl. Phys. Lett.* **67**, 3114 (1995). <https://doi.org/10.1063/1.114851>
- S.Y. Chou, P.R. Krauss, P.J. Renstrom, *Science* **272**, 85 (1996). <https://doi.org/10.1126/science.272.5258.85>
- L.J. Guo, *Adv. Mater.* **19**, 495 (2007). <https://doi.org/10.1002/adma.200600882>
- H. Tan, A. Gilbertson, S.Y. Chou, *J. Vac. Sci. Technol. B* **16**, 3926 (1998). <https://doi.org/10.1116/1.590438>
- D.K. Owens, R.C. Wendt, *J. Appl. Polym. Sci.* **13**, 1741 (1969). <https://doi.org/10.1002/app.1969.070130815>

**Publisher’s Note** Springer Nature remains neutral with regard to jurisdictional claims in published maps and institutional affiliations.